Biallelic *SUN5* Mutations Cause Autosomal-Recessive Acephalic Spermatozoa Syndrome

Fuxi Zhu,[1,2,3,*] Fengsong Wang,[3] Xiaoyu Yang,[4] Jingjing Zhang,[1,2] Huan Wu,[1,2] Zhou Zhang,[1,2] Zhiguo Zhang,[1,2,5] Xiaojin He,[1,2,5] Ping Zhou,[1,2,5] Zhaolian Wei,[1,2,5] Jozef Gecz,[6] and Yunxia Cao[1,2,5,*]

Acephalic spermatozoa syndrome is a rare and severe form of teratozoospermia characterized by a predominance of headless spermatozoa in the ejaculate. Family clustering and consanguinity suggest a genetic origin; however, causative mutations have yet to be identified. We performed whole-exome sequencing in two unrelated infertile men and subsequent variant filtering identified one homozygous (c.824C>T [p.Thr275Met]) and one compound heterozygous (c.1006C>T [p.Arg356Cys] and c.485T>A [p.Met162Lys]) *SUN5* (also named *TSARG4*) variants. Sanger sequencing of *SUN5* in 15 additional unrelated infertile men revealed four compound heterozygous (c.381delA [p.Val128Serfs*7] and c.824C>T [p.Thr275Met]; c.381delA [p.Val128Serfs*7] and c.781G>A [p.Val261Met]; c.216G>A [p.Trp72*] and c.1043A>T [p.Asn348Ile]; c.425+1G>A/c.1043A>T [p.Asn348Ile]) and two homozygous (c.851C>G [p.Ser284*]; c.350G>A [p.Gly114Arg]) variants in six individuals. These 10 *SUN5* variants were found in 8 of 17 unrelated men, explaining the genetic defect in 47.06% of the affected individuals in our cohort. These variants were absent in 100 fertile population-matched control individuals. *SUN5* variants lead to absent, significantly reduced, or truncated SUN5, and certain variants altered SUN5 distribution in the head-tail junction of the sperm. In summary, these results demonstrate that biallelic *SUN5* mutations cause male infertility due to autosomal-recessive acephalic spermatozoa syndrome.

Approximately 15% of couples have difficulties conceiving, and male factors are likely involved in half of these.[1] Teratozoospermia is the main cause of male infertility. Acephalic spermatozoa syndrome is an apparently rare and severe type of teratozoospermia causing male infertility. So far, more than 20 cases have been reported, and its genetic cause in humans remains unknown.[2–14] Semen from infertile men with this syndrome consistently shows nearly 100% abnormally shaped spermatozoa. The majority is comprised of headless tails, as well as a very small proportion of intact spermatozoa with an abnormal head-tail junction and also a few tailless heads. This syndrome has a typical ultrastructural anomaly involving the absence of the implantation fossa and basal plate between the sperm head and the tail. This sperm anomaly can be easily identified through detection of tailless heads, as well as of sperm with an abnormal head-tail junction.[7,10,11] As for the acephalic sperm, they contain a normally arranged proximal centriole and other components in the normal sperm tail.[7,10,11] This syndrome has been previously identified to be familial, and has also been found in a consanguineous family,[11,12] strongly suggesting genetic origin.[5,11,14] Whereas, in mice, loss of function of several genes (*Hook1*,[15] *Prss21*,[16] *Oaz3*,[17] *Cntrob*,[18] *Ift88*,[19] *Odf1*,[20,21] and *Spata6*[22]) can cause male infertility due to acephalic spermatozoa syndrome, no mutations of these genes have been identified in humans. This can be explained by either genetic heterogeneity underlying this syndrome or differing functions or molecular pathogenesis between mice and humans.[23] To identify the responsible gene variants in humans, we performed whole-exome sequencing (WES) in two unrelated infertile men with this syndrome and identified *SUN5* variants as the likely cause of the syndrome. Subsequent screening of 15 other unrelated affected individuals identified additional autosomal-recessive mutations, which were functionally assessed for loss-of-function effect.

Altogether, we have collected data from 17 infertile men with acephalic spermatozoa syndrome who were referred to us for primary infertility. We have evaluated all available clinical data. There were no previous records of significant illnesses, and complete andrological examinations of these individuals were normal. Numerous previous semen analyses revealed severe teratozoospermia. In all affected individuals, the predominant anomaly was acephalic spermatozoa, with a variable but low proportion of abnormal head-tail junctions and tailless heads (Figures 1A and 1B). Other semen parameters available for different individuals consisted of different amounts of oligozoospermia (less than 15×10^6 spermatozoa/mL) and asthenospermia (progressive motility of 0% in all cases) (Tables S1 and S2). Electron micrographs revealed acephalic spermatozoa (or decapitated tails) in all cases. The sperm otherwise contained a normally arranged proximal centriole and segmented columns (Figures 1C and 1E). The tailless heads (or decaudated heads) contained the nucleus, often enlarged, with or without a typical acrosome structure. Interestingly, all affected individuals had two consistent

[1]Reproductive Medicine Center, Department of Obstetrics and Gynecology, The First Affiliated Hospital of Anhui Medical University, Hefei 230022, China; [2]Institute of Reproductive Genetics, Anhui Medical University, Hefei 230022, China; [3]School of Life Science, Anhui Medical University, Hefei 230022, China; [4]Center of Clinical Reproductive Medicine, First Affiliated Hospital, Nanjing Medical University, Nanjing 210029, China; [5]Anhui Provincial Engineering Technology Research Center for Biopreservation and Artificial Organs, Hefei 230022, China; [6]School of Medicine, Robinson Research Institute, The University of Adelaide, and South Australian Health and Medical Research Institute, Adelaide, South Australia 5006, Australia
*Correspondence: fxzhu@ahmu.edu.cn (F.Z.), caoyunxia6@126.com (Y.C.)
http://dx.doi.org/10.1016/j.ajhg.2016.08.004.
© 2016 American Society of Human Genetics.

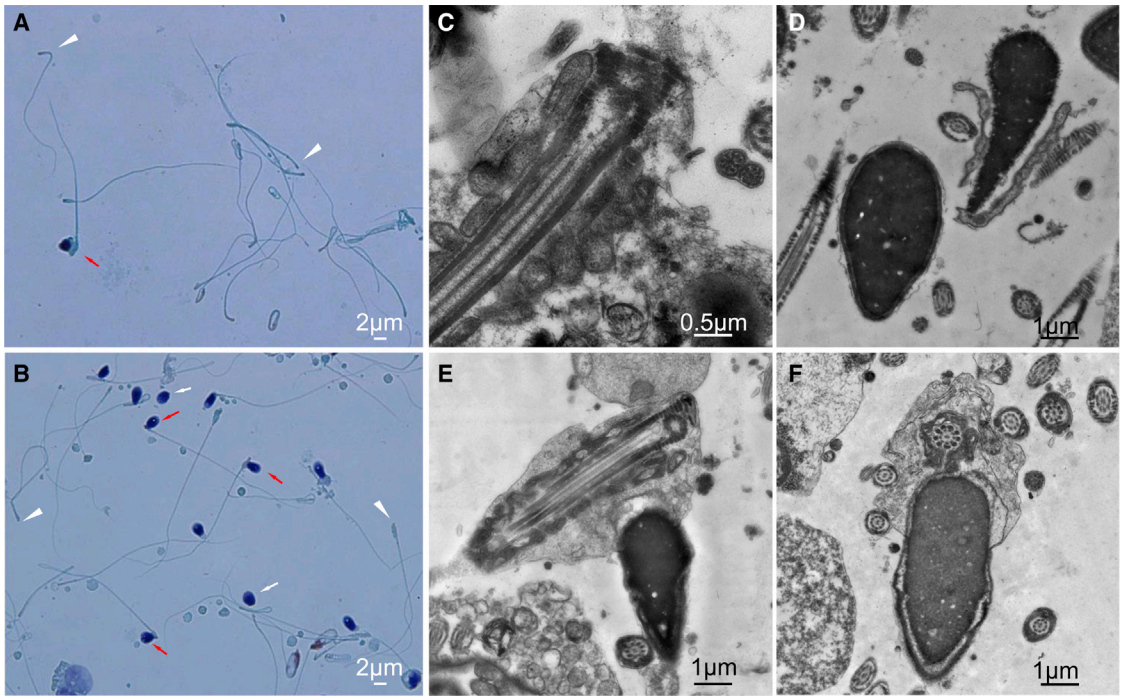

Figure 1. Analysis of the Sperm of Infertile Men with Acephalic Spermatozoa Syndrome Due to Mutations in *SUN5*
(A and B) Photomicrographs of ejaculated semen smear stained by Papanicolaou. The majority of the ejaculated spermatozoa are headless (white arrowhead). A small proportion of intact spermatozoa have an abnormal head-tail junction (red arrow), and a few tailless heads (white arrow) can be observed.
(C–F) Transmission electron micrographs of the representative spermatozoa. A headless spermatozoon contains the proximal centriole, segmented columns, mitochondria, and all the other components normally included in the tail (C). A tailless spermatozoon contains a slightly enlarged nucleus without a typical acrosome structure but lacks the implantation fossa and basal plate (D). A longitudinal section (E) and a cross section (F) of a spermatozoon with an abnormal head-tail junction show that the head is laterally inserted into the cytoplasmic residual body of the proximal tail. The head contains the nucleus and almost normally shaped acrosome but lacks the implantation fossa and basal plate at the caudal pole of the nucleus. The tail contains the proximal centriole, segmented columns, mitochondria (showed in C), and normally arranged axoneme (showed in C and E).

abnormalities: the absence of the implantation fossa and the basal plate (Figure 1D). The spermatozoa with abnormal head-tail junctions showed a nearly normal-shaped nucleus and acrosome but a lack of the implantation fossa and the basal plate in the head. The heads were attached to the tip or the sides of the midpiece without a linear alignment of the sperm axis, and angles of 90°–180° were frequently observed between the heads and tails (Figures 1E and 1F). No additional affected family members were identified among the relatives of these 17 unrelated individuals. However, 6 of our affected individuals (35.3%) were from consanguineous families. All of them had a normal karyotype (46, XY). DNA samples were obtained from all 17 individuals, 6 of whom also provided semen for western blotting and immunofluorescence studies. Additional semen samples for research purposes could not be obtained from any of the affected individuals. Testicular biopsies were not performed. Additionally, 100 DNA samples of unrelated, anonymous, male sperm donors from the same population were used as controls. Written informed consent was obtained from all participants. We have also used one human testis sample for RNA extraction from an individual with prostate cancer after obtaining oral consent from him. This individual was scheduled for bilateral castration as part of cancer treatment at the department of urology in the hospital. This study protocol was approved by the human research ethics committee of our hospital and the university.

We performed WES in two unrelated infertile men with this syndrome who were initially referred to us for infertility. Genomic DNA library was captured and enriched with the SureSelect Human All Exon V5 (Agilent), according to the manufacture's protocol. Exome sequencing was performed on the HiSeq2000 sequencing platform (Illumina). Sequenced reads were collected, filtered for quality, and aligned to the human reference sequence (UCSC Genome Browser hg19) with the Burrows-Wheeler Aligner.[24] Genotypes were called by SAMtools,[25] Picard, and GATK. Sequence variants including single-nucleotide variants (SNVs) and small insertions or deletions (indels) were annotated by ANNOVAR software.[26] Common variants (defined as 10% frequency in 1000 Genomes) were excluded if they were present in the dbSNP (v.138 and v.142) database, the 1000 Genomes Project, the HapMap CHB (Han Chinese in Beijing, China) population, the National Heart, Lung, and Blood Institute Exome Sequencing Project (ESP) Exome Variant Server (EVS), or the Exome Aggregation Consortium (ExAC) Browser.

SNVs and indels were classified by position as intergenic, 5′ UTR, 3′ UTR, intronic, splicing, or exonic. Exonic variants were then classified by predicted amino acid change as a stopgain, missense, synonymous, or frameshift variant, inframe insertion or deletion, or possible splice-site mutation (Table S3). For coding or splice-site mutations, the conservation at the variant site and the predicted effect on protein function were evaluated with in silico tools SIFT,[27] PolyPhen-2,[28] MutationTaster,[29] and NNSplice.[30] Initially, we filtered genes that had predicted deleterious variants in both unrelated affected individuals. Full whole-exome data of both individuals are available upon request.

On the basis of the family pedigrees and clinical observations, we postulated an autosomal-recessive genetic model for this syndrome (Figure 2A). In family 1 (F1), the affected male is an offspring of a consanguineous marriage. To identify the likely responsible genetic variant(s) for this individual, F1:II-3, we focused on homozygous, identical-by-descent, predicted-to-be-damaging variants. There were three variants fulfilling this criterion: an acceptor splice-site variant in *DDX31* (MIM: 616533), a missense variant in *WDFY2* (MIM: 610418), and a missense variant in *SUN5* (MIM: 613942) (Table S4). Both *WDFY2* and *SUN5* were within two larger (>1 Mb) and thus likely identical-by-descent homozygous intervals (Table S3). Subsequently, we filtered and prioritized variants of individual II-4, from a non-consanguineous family (family 2 [F2]), to identify homozygous or compound heterozygous variants. No potentially damaging homozygous variants were detected. However, 11 compound heterozygous missense variants in five genes—*LONRF2*, *ZDHHC24*, *HELZ2* (MIM: 611265), *DNAH17* (MIM: 610063), and *SUN5*—fulfilled this criterion (Table S5). Because *SUN5* variants were identified in both families, *SUN5* (also called *TSARG4* or *SPAG4L*[31,32]) seemed the most appropriate candidate gene for this infertility syndrome.

The homozygous *SUN5* (GenBank: NM_080675.3) missense variant identified in individual F1:II-3, c.824C>T (p.Thr275Met), alters a highly conserved amino acid residue and is predicted to be highly damaging (Table 1). The unaffected parents and two sisters were heterozygous carriers for the variant (Figure 2A). Compound heterozygous missense variants were identified in individual F2:II-4, (c.1066C>T [p.Arg356Cys] and c.485T>A [p.Met162Lys]). Both variants disrupted highly conserved amino acids (Figure S1), and these substitutions are predicted to be highly damaging (Table 1). The affected individual inherited the c.1066C>T allele from his heterozygous father and the c.485T>A allele from his mother. One sister also carries the c.485T>A allele, and neither of these variants was detected in the unaffected brother.

Subsequently we screened 15 other unrelated individuals with a similar type of infertility by Sanger sequencing (primers in Table S6) and found candidate *SUN5* variants in six of them. Four of these individuals had compound heterozygous variants and two had homozygous variants (Figure 2A and Table 1). Segregation analysis could not be performed in the consanguineous family 8, with homozygous variant c.340G>A (p.Gly114Arg), because parental DNA was not available. Other variants identified in families 3–7 were all heterozygous in corresponding individuals' parents and segregated in these families as expected (Figure 2A). The c.425+1G>A splice-site variant is predicted by NNSplice[30] to abolish the donor splice site of intron 7. The splice-site variant c.425+1G>A, the frameshift variant c.381delA, and the two nonsense variants c.216G>A and c.851C>G are predicted to be loss-of-function variants leading to a premature termination codon (PTC) in *SUN5* mRNA. Such PTC-containing mRNA is predicted to be degraded by nonsense-mediated mRNA decay (NMD).[33] The nonsynonymous variant c.340G>A (p.Gly114Arg) was predicted by NNSplice[30] to abolish the donor splice site in intron 5, leading to either a partial or whole retention of intron 5 or skipping of exon 5, either of which would introduce a PTC in the *SUN5* mRNA and lead to a complete loss of SUN5. Furthermore, SUN5 is a 379-amino-acid transmembrane protein located in the inner nuclear membrane (INM) [31,32] and composed of an N-terminal nucleoplasmic region, one transmembrane helix, a coiled-coil region, and a SUN-domain region in the C terminus (Figure 2B). If c.340G>A is not causing a splicing problem, the resulting missense change p.Gly114Arg is predicted to severely impair the transmembrane helix of SUN5 (by PSORTII and TMHMM), with predicted loss of SUN5 from the nuclear envelope (NE) during spermatogenesis. The missense variant p.Met162Lys is predicted to disturb the localization of SUN5 to the NE through the impairment of the coiled-coil structure, whereas p.Val261Met, p.Thr275Met, p.Asn348Ile, and p.Arg356Cys, located in the C-terminal SUN domain, would disturb the interaction of SUN with its partners (uncharacterized proteins) in the perinuclear space (PNS)[34] (Figure 2B).

All ten variants were absent from the DNA of 100 (200 chromosomes) control fertile men from the same population. *SUN5* has a residual variation intolerance score[35] of −0.27 (corresponding to the top 34.71% of the human genes most intolerant to genetic variation). However, constraint metrics reported in the ExAC Browser indicated that *SUN5* is tolerant to both heterozygous loss-of-function (probability of loss-of-function intolerance = 0.00) and heterozygous missense (Z score = −0.03) mutations, which indicates that *SUN5* has more heterozygous variants in general populations than expected. Interestingly, inspection of the ExAC dataset (n > 60,117 exomes) (Table 1) identified five of ten of these *SUN5* variants as having a low allele frequency (<27/121,228), and not only in the Asian population but also in non-Asian populations. However, none of these variants was present in a homozygous state. We also noticed that *SUN5* has other loss-of-function ExAC variants in Asians as well as non-Asians. This suggests that *SUN5* mutations contribute to male infertility in non-Asian populations as well.

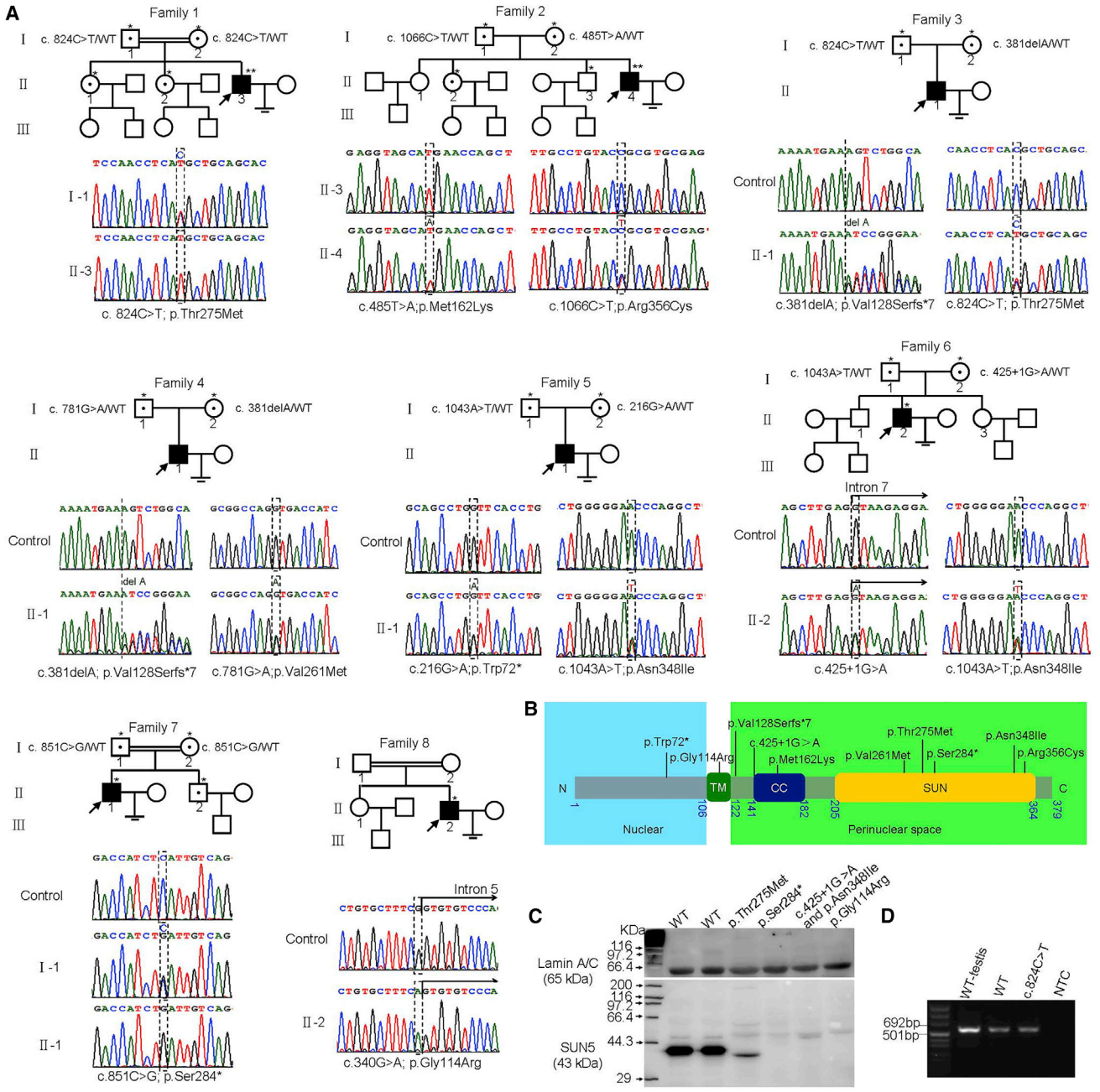

Figure 2. Pedigrees and *SUN5* Mutations in Families Affected by Acephalic Spermatozoa Syndrome

(A) Pedigrees of the eight families with inherited *SUN5* mutations are shown. The individuals with a single star were Sanger sequenced. Individuals F1:II-3 and F2:II-4 were tested by WES (two stars).

(B) The domain architecture of SUN5 and the location of the SUN5 variants. The protein has 379 amino acids (gray) and contains a single transmembrane (TM) domain (green), a coiled-coil (CC) domain (blue), and a SUN domain (yellow). SUN5 is located on the inner nuclear membrane; the N terminus is in the nuclear space (light-blue background), and the C terminus extends to the perinuclear space (light-green background).

(C) Western blot showing Lamin A/C (Proteintech antibodies, 10298-1-AP) and SUN5 (Proteintech antibodies, 17495-1-AP) levels on ejaculated sperm from two control individuals and four affected individuals with SUN5 variants. Molecular weights, showed in the left lane, were determined according to the protein molecular weight marker (Takara, broad range, 3452Q).

(D) Agarose gel image of cDNA PCR products encompassing exons 10–13 of *SUN5* (forward primer 5′-CCTGAAGTCTATAGGGGCCA-3′; reverse primer 5′-ATCTCTCTTAGGGTAGGGGTTC-3′). A single band of expected size was detected in individual F1:II-3, with the c.824C>T (p.Thr275Met) mutation, suggesting that this variant does not affect splicing. WT testis is a sample from an individual with prostate cancer who underwent bilateral castration treatment. NTC represents negative control.

SUN5 is specifically expressed in testes,[31,32,36] so we assessed SUN5 amount and distribution in available semen samples. SUN5 amounts were significantly lower and the protein appeared to be slightly shorter in individual F1:II-3, with the p.Thr275Met variant, than in control individuals (Figure 2C). We excluded the possibility that

Table 1. Effects of *SUN5* Mutations, Predicted with In Silico Tools

Chromosome 20 Coordinates	cDNA Alteration	Amino Acid Alteration	Exon	Mutation	ExAC Allele Frequency	ExAC Homozygotes Frequency	NNSplice	SIFT	PolyPhen-2	MutationTaster
31,573,615G>A	c.824C>T	p.Thr275Met	11	missense	4/121,306	0/121,306	–	0.00 (D)	0.999 (D)	1.000 (D)
31,571,674G>A	c.1066C>T	p.Arg356Cys	13	missense	6/121,306	0/121,306	–	0.00 (D)	0.999 (D)	1.000 (D)
31,583,474A>T	c.485T>A	p.Met162Lys	8	missense	not found	not found	–	0.02 (D)	0.042 (B)	0.778 (N)[b]
31,585,452CT>C	c.381delA	p.Val128Serfs*7	6	frameshift	27/121,228	0/121,228	–	–	–	1.000 (D)
31,573,658C>T	c.781G>A	p.Val261Met	11	missense	not found	not found	–	0.04 (D)	0.999 (D)	0.987 (D)
31,589,080C>T	c.216G>A	p.Trp72*	4	nonsense	not found	not found	–	–	–	1.000 (D)
31,571,697T>A	c.1043A>T	p.Asn348Ile	13	missense	9/120,234	0/120,234	–	0.01 (D)	0.985 (D)	0.993 (D)
31,584,129C>T	c.425+1G>A	–	7	splice site	2/121,152	0/121,152	1.00 to <0.10[a]	–	–	1.000 (D)
31,573,588G>C	c.851C>G	p.Ser284*	11	nonsense	not found	not found	–	–	–	1.000 (D)
31,587,880C>T	c.340G>A	p.Gly114Arg	5	splice site	not found	not found	0.52 to <0.10[a]	0.35 (T)	0.954 (D)	0.990 (D)

(D), deleterious; (N), neutral; (T), tolerated; (B), benign.
[a]The mutations c.425+1G>A and p.Gly114Arg were predicted to cause loss of a donor splice site.
[b]The mutation p.Met162Lys was predicted by MutationTaster to cause loss of coil structure.

this variant affects splicing by RT-PCR (Figure 2D); however, we did not examine posttranslational modification. The p.Ser284* (F7:II-1), c.425+1G>A and p.Asn348Ile (F6:II-1), and p.Gly114Arg (F8:II-2) variants were nearly undetectable (Figure 2C). In a control sample, SUN5 was localized to the head-tail junction of the sperm, although there is some non-specific staining in the regions of the sperm head and tail in the affected and control individuals (Figure 3). This is consistent with a previous publication.[36] SUN5 could not be detected in the head-tail junction of sperm in individuals with SUN5 mutations. SUN5 amounts and distribution pattern were normal in the ejaculated sperm of two affected individuals in whom no *SUN5* mutation was identified (Figures S2 and S3), helping to exclude the possibility that the absence of SUN5 in the head-tail junction of the sperm could be secondary to or caused by the destruction of the sperm-head junction.

SUN5 is synthesized in the endoplasmic reticulum (ER), transits to the Golgi apparatus, reaches the NE and attaches to the INM, and finally moves to the junction area between the sperm head and tail.[36] We speculated that the variants we identified would disturb this dynamic distribution of SUN5, leaving SUN5 susceptible to being discarded through the residual body (a giant vesicle transformed from most membrane compartments of the spermatic cytoplasm) at the end of the spermatozoon differentiation.[37]

Acephalic spermatozoa have a typical ultrastructural anomaly—the absence of the implantation fossa and the basal plate.[7,10,11] Given the fragile head-tail junction, the sperm heads and tails start to be separated within the seminiferous tubules of testes or during their transition through the seminal tract.[2,5] The formation of the implantation fossa and the basal plate could be a highly regulated process. LINC complexes (linkers of the nucleoskeleton to the cytoskeleton), which tether nuclei to different cytoskeletal elements, might be involved. They are composed of SUN proteins on the INM and KASH proteins (Klarsicht, ANC-1, and Syne [also known as Nesprin] homology) on the outer nuclear membrane.[34,36–41] The N-terminal nucleoplasmic region of the SUN proteins binds to the nucleoskeletal elements and chromatin, the C-terminal SUN domain extends to the PNS and directly interacts with the C-terminal KASH domain of the KASH proteins, and the N terminus of the KASH protein interacts with different cytoskeleton proteins. In mammals, five different members of the SUN-domain protein family were identified: SUN1, SUN2, SUN3, SUN4 (or, SPAG4), and SUN5 (or, SPAG4L).[31,32,39–41] *SUN5* was specifically expressed in testes.[31,32,36] SUN5 was distributed in the head-tail junction, exactly in front of the implantation fossa, in epididymal sperm. This special pattern of SUN5 distribution was already observable in late condensing spermatids.[36] Therefore, SUN5 was a strong functional and structural candidate to participate in head-tail attachment.

In this study, we have identified ten different *SUN5* variants that we predicted to be disease causing. These

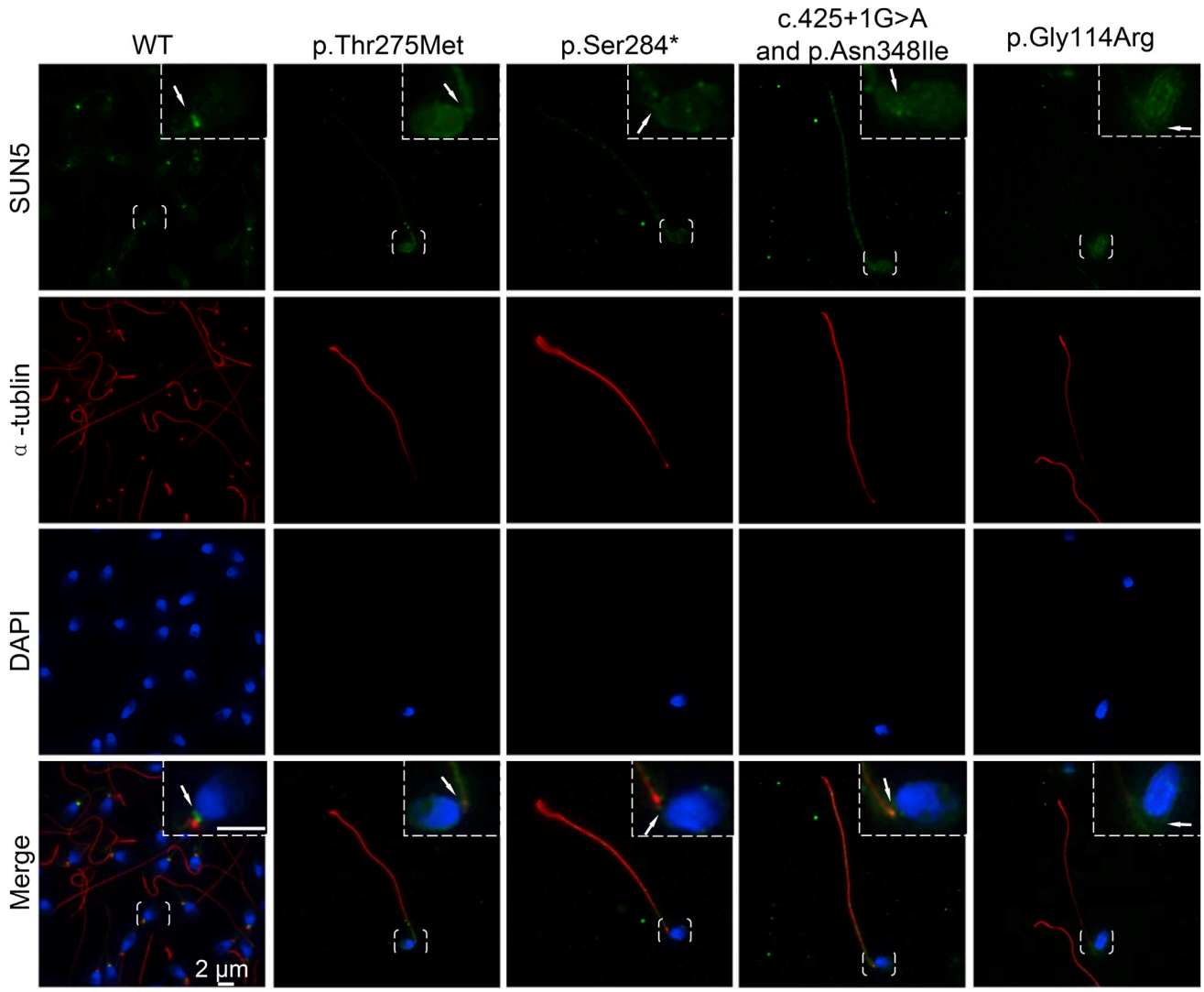

Figure 3. The Consequences of *SUN5* Mutations on Protein Distribution in Sperm
SUN5 immunofluorescence in sperm from control (WT) and affected individuals. SUN5 staining is confined to the head-tail junction region (exactly in the distal part of the inner nuclear membrane, which is close to the distal end of the nucleus) in control sperm (highlighted by white arrow). This specific pattern of distribution is not observed in abnormal head-tail junction spermatozoon of affected individuals with *SUN5* mutations. Anti-α-tubulin antibody staining paints the tails of the sperm, and DAPI indicates the nucleus in the sperm head. The scale is shown at the bottom left panel. (Inset) Digital enlargement of the respective sperm head-tail junction regions.

include two nonsense, one frameshift, two splice-site, and five missense mutations (Table 1), identified in 8 of 17 unrelated individuals (47.06%). We show that at least some of the *SUN5* mutations lead to a loss of SUN5. The mechanism of action of the missense mutations was not further determined. However, given that there were no major clinical differences ($p > 0.05$) among the infertile men with these missense mutations and those with loss-of-function mutations (Table S2), we predict that all mutations identified lead to loss-of-function of SUN5. Identification of additional affected individuals and mutations will help to address the underlying mechanism. As for the five missense mutations, four are located within the C-terminal SUN domain of SUN5 and might severely disrupt the interaction of SUN5 with its partners, such as some uncharacterized KASH or LINC proteins. One missense variant, p.Met162Lys, is located in the coiled-coil domain and might disturb the localization of SUN5 to the NE and to the region of head-tail junction. We hypothesize that SUN5 variants disturb the formation of its corresponding LINC complexes, causing disassociation between the nucleoskeleton and the cytoskeleton, or disturb the localization of the SUN5 to the NE. Given that SUN5 is located in the distal part of the INM or in front of the implantation fossa, we propose that this disassociation might disrupt the formation of the implantation fossa and the basal plate and cause further anomaly of the head-tail junction, which could be fragile enough to cause sperm heads and tails to detach.

In conclusion, our results determine that acephalic spermatozoa syndrome can be caused by recessive loss-of-function mutations of *SUN5*. These findings will allow precise genetic diagnosis of acephalic spermatozoa syndrome in Asian and non-Asian populations and facilitate genetic counseling for reproductive options.

Supplemental Data

Supplemental Data include three figures and six tables and can be found with this article online at http://dx.doi.org/10.1016/j.ajhg.2016.08.004.

Acknowledgments

We would like to thank all families for participating in this study. We are thankful to Jianzhong Wang from the Department of Urology at the First Affiliated Hospital of Anhui Medical University for providing a testis sample and to Wen Hu from Anhui Provincial Hospital and Qin Wang from Anhui Agricultural University for electron microscopy techniques. This study was supported by the National Natural Science Foundation of China (81401251 to F.Z.) and by The Key Program in the Youth Elite Support Plan in Universities of Anhui Province (gxyqZD2016050 to F.Z.).

Received: May 25, 2016
Accepted: August 5, 2016
Published: September 15, 2016

Web Resources

1000 Genomes, http://www.1000genomes.org
Berkeley Drosophila Genome Project NNSplice 0.9, http://www.fruitfly.org/seq_tools/splice.html
ExAC Browser, http://exac.broadinstitute.org/
GenBank, http://www.ncbi.nlm.nih.gov/genbank/
International HapMap Project, http://hapmap.ncbi.nlm.nih.gov/
MutationTaster, http://www.mutationtaster.org/
NHLBI Exome Sequencing Project (ESP) Exome Variant Server, http://evs.gs.washington.edu/EVS/
OMIM, http://www.omim.org/
PolyPhen-2, http://genetics.bwh.harvard.edu/pph2/
PSORTII Prediction, http://psort.hgc.jp/form2.html
SIFT, http://sift.bii.a-star.edu.sg/
TMHMM, http://www.cbs.dtu.dk/services/TMHMM/

References

1. Mascarenhas, M.N., Flaxman, S.R., Boerma, T., Vanderpoel, S., and Stevens, G.A. (2012). National, regional, and global trends in infertility prevalence since 1990: a systematic analysis of 277 health surveys. PLoS Med. *9*, e1001356.
2. Perotti, M.E., Giarola, A., and Gioria, M. (1981). Ultrastructural study of the decapitated sperm defect in an infertile man. J. Reprod. Fertil. *63*, 543–549.
3. Baccetti, B., Selmi, M.G., and Soldani, P. (1984). Morphogenesis of 'decapitated' spermatozoa in a man. J. Reprod. Fertil. *70*, 395–397.
4. Chemes, H.E., Carizza, C., Scarinci, F., Brugo, S., Neuspiller, N., and Schwarsztein, L. (1987). Lack of a head in human spermatozoa from sterile patients: a syndrome associated with impaired fertilization. Fertil. Steril. *47*, 310–316.
5. Baccetti, B., Burrini, A.G., Collodel, G., Magnano, A.R., Piomboni, P., Renieri, T., and Sensini, C. (1989). Morphogenesis of the decapitated and decaudated sperm defect in two brothers. Gamete Res. *23*, 181–188.
6. Toyama, Y., Kazama, T., Fuse, H., and Katayama, T. (1995). A case of decapitated spermatozoa in an infertile man. Andrologia *27*, 165–170.
7. Chemes, H.E., Puigdomenech, E.T., Carizza, C., Olmedo, S.B., Zanchetti, F., and Hermes, R. (1999). Acephalic spermatozoa and abnormal development of the head-neck attachment: a human syndrome of genetic origin. Hum. Reprod. *14*, 1811–1818.
8. Saïas-Magnan, J., Metzler-Guillemain, C., Mercier, G., Carles-Marcorelles, F., Grillo, J.M., and Guichaoua, M.R. (1999). Failure of pregnancy after intracytoplasmic sperm injection with decapitated spermatozoa: case report. Hum. Reprod. *14*, 1989–1992.
9. Kamal, A., Mansour, R., Fahmy, I., Serour, G., Rhodes, C., and Aboulghar, M. (1999). Easily decapitated spermatozoa defect: a possible cause of unexplained infertility. Hum. Reprod. *14*, 2791–2795.
10. Toyama, Y., Iwamoto, T., Yajima, M., Baba, K., and Yuasa, S. (2000). Decapitated and decaudated spermatozoa in man, and pathogenesis based on the ultrastructure. Int. J. Androl. *23*, 109–115.
11. Porcu, G., Mercier, G., Boyer, P., Achard, V., Banet, J., Vasserot, M., Melone, C., Saias-Magnan, J., D'Ercole, C., Chau, C., and Guichaoua, M.R. (2003). Pregnancies after ICSI using sperm with abnormal head-tail junction from two brothers: case report. Hum. Reprod. *18*, 562–567.
12. Rondanino, C., Duchesne, V., Escalier, D., Jumeau, F., Verhaeghe, F., Peers, M.C., Mitchell, V., and Rives, N. (2015). Evaluation of sperm nuclear integrity in patients with different percentages of decapitated sperm in ejaculates. Reprod. Biomed. Online *31*, 89–99.
13. Gambera, L., Falcone, P., Mencaglia, L., Collodel, G., Serafini, F., De Leo, V., and Piomboni, P. (2010). Intracytoplasmic sperm injection and pregnancy with decapitated sperm. Fertil Steril *93*, 1347 e1347-1312.
14. Moretti, E., Geminiani, M., Terzuoli, G., Renieri, T., Pascarelli, N., and Collodel, G. (2011). Two cases of sperm immotility: a mosaic of flagellar alterations related to dysplasia of the fibrous sheath and abnormalities of head-neck attachment. Fertil. Steril. *95*, e19–23.
15. Mendoza-Lujambio, I., Burfeind, P., Dixkens, C., Meinhardt, A., Hoyer-Fender, S., Engel, W., and Neesen, J. (2002). The Hook1 gene is non-functional in the abnormal spermatozoon head shape (azh) mutant mouse. Hum. Mol. Genet. *11*, 1647–1658.
16. Netzel-Arnett, S., Bugge, T.H., Hess, R.A., Carnes, K., Stringer, B.W., Scarman, A.L., Hooper, J.D., Tonks, I.D., Kay, G.F., and Antalis, T.M. (2009). The glycosylphosphatidylinositol-anchored serine protease PRSS21 (testisin) imparts murine epididymal sperm cell maturation and fertilizing ability. Biol. Reprod. *81*, 921–932.
17. Tokuhiro, K., Isotani, A., Yokota, S., Yano, Y., Oshio, S., Hirose, M., Wada, M., Fujita, K., Ogawa, Y., Okabe, M., et al. (2009). OAZ-t/OAZ3 is essential for rigid connection of sperm tails to heads in mouse. PLoS Genet. *5*, e1000712.
18. Liska, F., Gosele, C., Rivkin, E., Tres, L., Cardoso, M.C., Domaing, P., Krejcí, E., Snajdr, P., Lee-Kirsch, M.A., de Rooij, D.G.,

et al. (2009). Rat hd mutation reveals an essential role of centrobin in spermatid head shaping and assembly of the head-tail coupling apparatus. Biol. Reprod. *81*, 1196–1205.
19. Kierszenbaum, A.L., Rivkin, E., Tres, L.L., Yoder, B.K., Haycraft, C.J., Bornens, M., and Rios, R.M. (2011). GMAP210 and IFT88 are present in the spermatid golgi apparatus and participate in the development of the acrosome-acroplaxome complex, head-tail coupling apparatus and tail. Dev. Dyn. *240*, 723–736.
20. Yang, K., Meinhardt, A., Zhang, B., Grzmil, P., Adham, I.M., and Hoyer-Fender, S. (2012). The small heat shock protein ODF1/HSPB10 is essential for tight linkage of sperm head to tail and male fertility in mice. Mol. Cell. Biol. *32*, 216–225.
21. Yang, K., Grzmil, P., Meinhardt, A., and Hoyer-Fender, S. (2014). Haplo-deficiency of ODF1/HSPB10 in mouse sperm causes relaxation of head-to-tail linkage. Reproduction *148*, 499–506.
22. Yuan, S., Stratton, C.J., Bao, J., Zheng, H., Bhetwal, B.P., Yanagimachi, R., and Yan, W. (2015). Spata6 is required for normal assembly of the sperm connecting piece and tight head-tail conjunction. Proc. Natl. Acad. Sci. USA *112*, E430–E439.
23. Vogt, P.H. (2004). Molecular genetics of human male infertility: from genes to new therapeutic perspectives. Curr. Pharm. Des. *10*, 471–500.
24. Li, H., and Durbin, R. (2009). Fast and accurate short read alignment with Burrows-Wheeler transform. Bioinformatics *25*, 1754–1760.
25. Li, H., Handsaker, B., Wysoker, A., Fennell, T., Ruan, J., Homer, N., Marth, G., Abecasis, G., and Durbin, R.; 1000 Genome Project Data Processing Subgroup (2009). The Sequence Alignment/Map format and SAMtools. Bioinformatics *25*, 2078–2079.
26. Wang, K., Li, M., and Hakonarson, H. (2010). ANNOVAR: functional annotation of genetic variants from high-throughput sequencing data. Nucleic Acids Res. *38*, e164.
27. Ng, P.C., and Henikoff, S. (2003). SIFT: Predicting amino acid changes that affect protein function. Nucleic Acids Res. *31*, 3812–3814.
28. Adzhubei, I.A., Schmidt, S., Peshkin, L., Ramensky, V.E., Gerasimova, A., Bork, P., Kondrashov, A.S., and Sunyaev, S.R. (2010). A method and server for predicting damaging missense mutations. Nat. Methods *7*, 248–249.
29. Schwarz, J.M., Cooper, D.N., Schuelke, M., and Seelow, D. (2014). MutationTaster2: mutation prediction for the deep-sequencing age. Nat. Methods *11*, 361–362.
30. Reese, M.G., Eeckman, F.H., Kulp, D., and Haussler, D. (1997). Improved splice site detection in Genie. J. Comput. Biol. *4*, 311–323.
31. Jiang, X.Z., Yang, M.G., Huang, L.H., Li, C.Q., and Xing, X.W. (2011). SPAG4L, a novel nuclear envelope protein involved in the meiotic stage of spermatogenesis. DNA Cell Biol. *30*, 875–882.
32. Frohnert, C., Schweizer, S., and Hoyer-Fender, S. (2011). SPAG4L/SPAG4L-2 are testis-specific SUN domain proteins restricted to the apical nuclear envelope of round spermatids facing the acrosome. Mol. Hum. Reprod. *17*, 207–218.
33. Mendell, J.T., Sharifi, N.A., Meyers, J.L., Martinez-Murillo, F., and Dietz, H.C. (2004). Nonsense surveillance regulates expression of diverse classes of mammalian transcripts and mutes genomic noise. Nat. Genet. *36*, 1073–1078.
34. Kracklauer, M.P., Link, J., and Alsheimer, M. (2013). LINCing the nuclear envelope to gametogenesis. Curr. Top. Dev. Biol. *102*, 127–157.
35. Petrovski, S., Wang, Q., Heinzen, E.L., Allen, A.S., and Goldstein, D.B. (2013). Genic intolerance to functional variation and the interpretation of personal genomes. PLoS Genet. *9*, e1003709.
36. Yassine, S., Escoffier, J., Abi Nahed, R., Pierre, V., Karaouzene, T., Ray, P.F., and Arnoult, C. (2015). Dynamics of Sun5 localization during spermatogenesis in wild type and Dpy19l2 knock-out mice indicates that Sun5 is not involved in acrosome attachment to the nuclear envelope. PLoS ONE *10*, e0118698.
37. Breucker, H., Schäfer, E., and Holstein, A.F. (1985). Morphogenesis and fate of the residual body in human spermiogenesis. Cell Tissue Res. *240*, 303–309.
38. Ray, P.F., Coutton, C., and Arnoult, C. (2016). Sun proteins and Dpy19l2 forming LINC-like links are critical for spermiogenesis. Biol. Open *5*, 535–536.
39. Göb, E., Schmitt, J., Benavente, R., and Alsheimer, M. (2010). Mammalian sperm head formation involves different polarization of two novel LINC complexes. PLoS ONE *5*, e12072.
40. Calvi, A., Wong, A.S., Wright, G., Wong, E.S., Loo, T.H., Stewart, C.L., and Burke, B. (2015). SUN4 is essential for nuclear remodeling during mammalian spermiogenesis. Dev. Biol. *407*, 321–330.
41. Pasch, E., Link, J., Beck, C., Scheuerle, S., and Alsheimer, M. (2015). The LINC complex component Sun4 plays a crucial role in sperm head formation and fertility. Biol. Open *4*, 1792–1802.

The American Journal of Human Genetics, Volume *99*

Supplemental Data

Biallelic *SUN5* Mutations Cause Autosomal-Recessive Acephalic Spermatozoa Syndrome

Fuxi Zhu, Fengsong Wang, Xiaoyu Yang, Jingjing Zhang, Huan Wu, Zhou Zhang, Zhiguo Zhang, Xiaojin He, Ping Zhou, Zhaolian Wei, Jozef Gecz, and Yunxia Cao

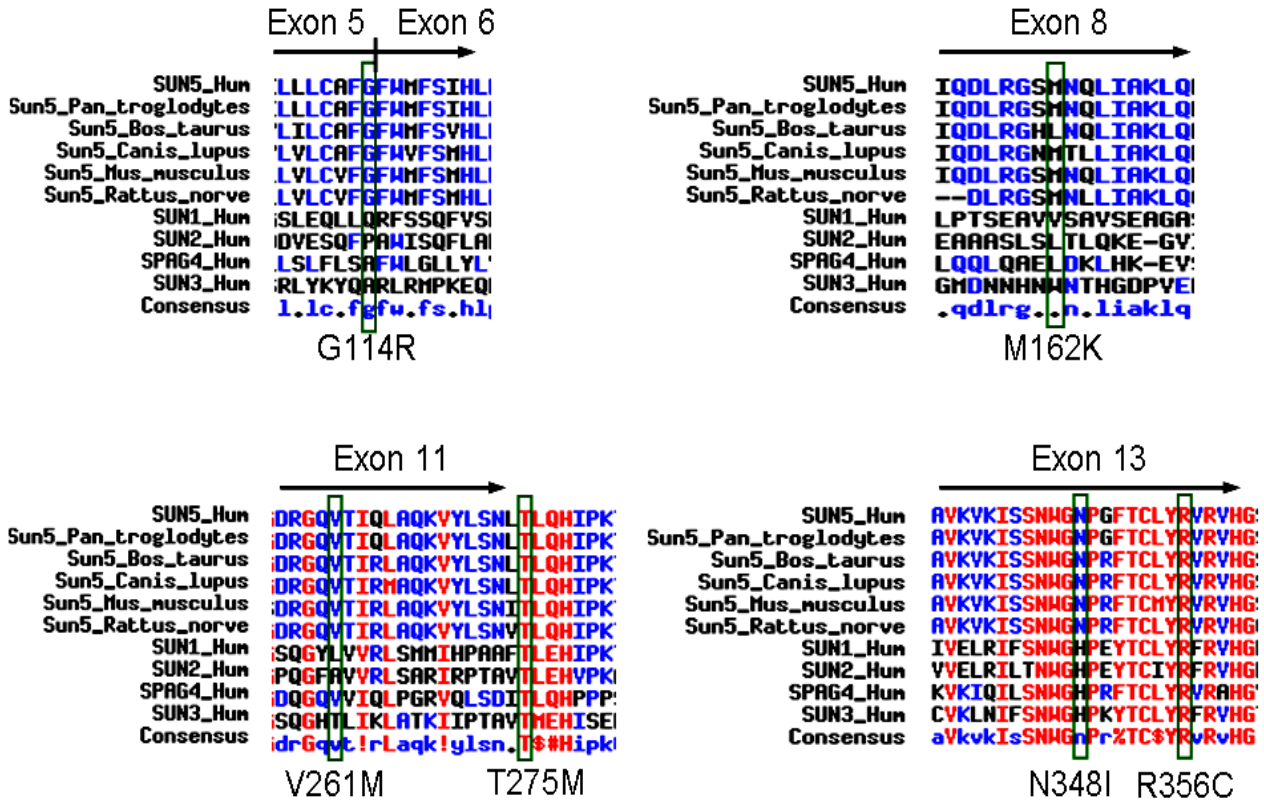

Figure S1

Conservation of SUN5 amino acid residues affected by missense mutations in the affected individuals with acephalic spermatozoa syndrome.

Partial amino acid sequence alignments across exons 5, 6, 8, 11 and 13 of selected SUN5 orthologs and paralogs are shown. The multiple sequence alignments have been performed using MultAlin. The amino acids in positions p.Gly114, p.Met162, p.Val261, p.Thr275, p.Asn348 and p.Arg356 are highlighted by a green rectangle.

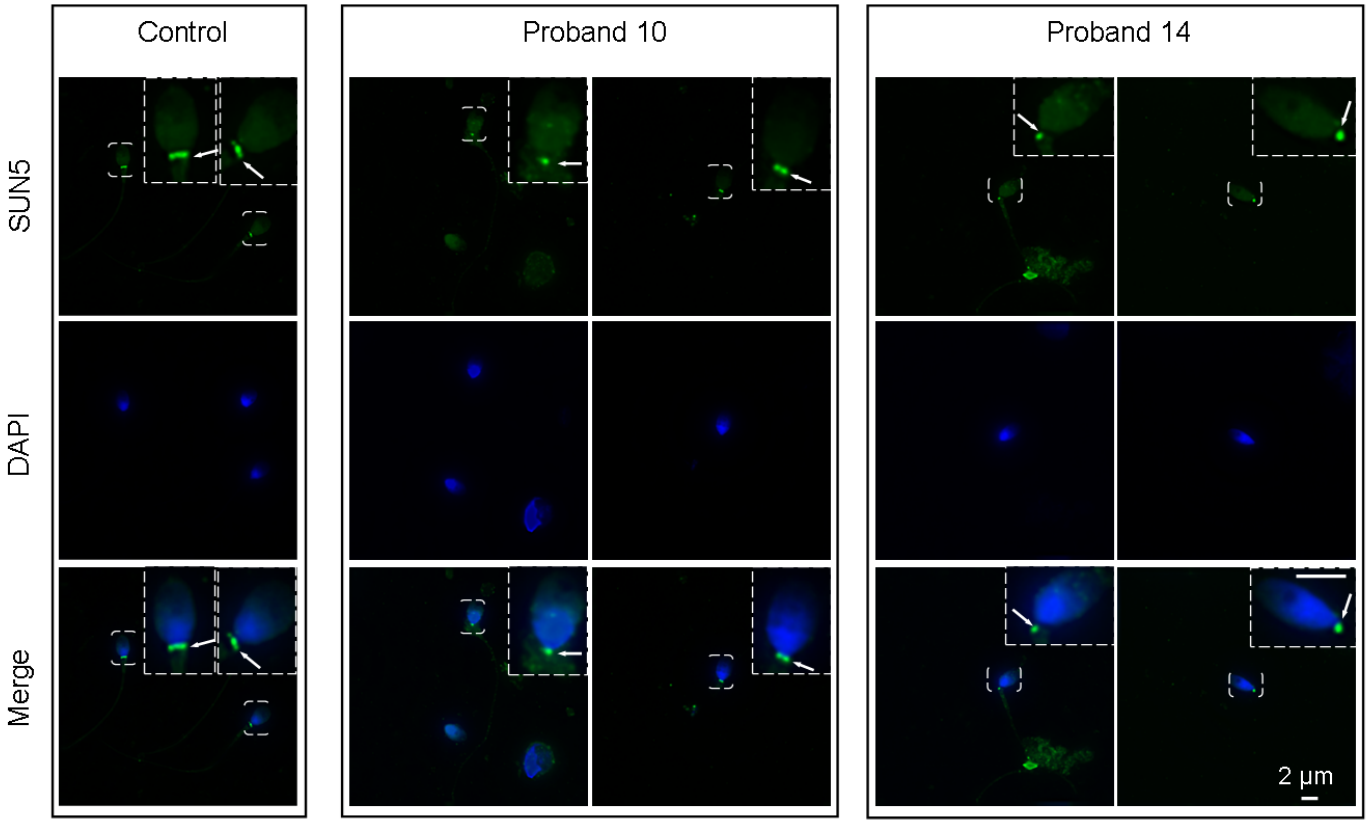

Figure S2

SUN5 immunofluorescence in sperm from controls and two affected individuals with acephalic spermatic syndrome without *SUN5* mutations.

SUN5 staining is confined to the head-tail junction region (exactly in the distal part of the inner nuclear membrane which is close to the distal end of the nucleus) in control sperm (highlighted by white arrow). This specific pattern of distribution is not changed in abnormal head-tail junction sperm (left panel) or in acephalic sperm (right panel) of two affected individuals (Proband 10 and Proband 14) with no *SUN5* mutations. DAPI indicates the nucleus in the sperm head. The scale is shown at the bottom right panel. (*Insets*) Digital enlargement of the respective sperm head-tail junction regions.

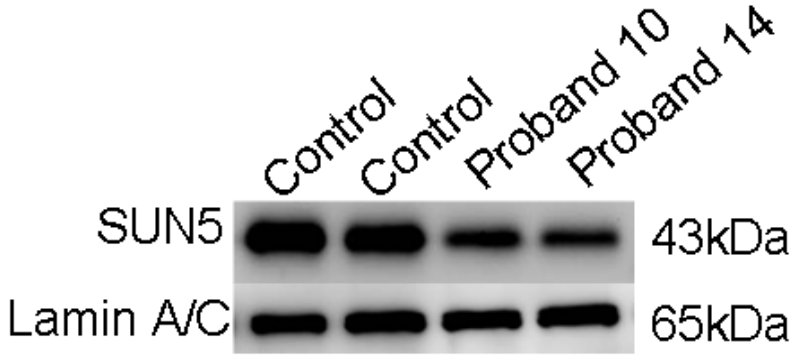

Figure S3

SUN5 levels in two affected individuals with acephalic spermatic syndrome without *SUN5* mutations.

Western blot showing SUN5 (Proteintech antibodies, 17495-1-AP) on ejaculated sperm from two controls and from two affected individuals (Proband 10 and Proband 14) with no *SUN5* variants identified.

Table S1. Semen parameters of affected individuals with acephalic spermatozoa syndrome grouped by *SUN5* genotype.

Mutation types	**M / M**		**– / M**				**– / –** [a]		**No MT**								
Patients	**F1:II-3**	**F2:II-4**	**F3:II-1**	**F4:II-1**	**F5:II-1**	**F6:II-2**	**F7:II-1**	**F8:II-2**	**P9**[b]	**P10**	**P11**	**P12**	**P13**	**P14**	**P15**	**P16**	**P17**
volume (ml)	2.2[c]	3.3	3.9	1.9	3.0	1.2	1.8	2.8	3.3	2.7	3.6	3.1	1.2	1.1	2.8	2.1	3.8
Concentration [d]	5.3	3.2	1.5	10.8	3.7	7.6	6.5	4.9	2.2	3.3	2.3	3.4	6.8	9.2	3.8	5.5	2.5
Motility B+C (%) [e]	23.4	18.4	18.3	16.1	8.6	3.6	20.2	26.4	8.9	4.2	14.6	28.8	20.4	13.6	7.2	6.4	19.4
Percentages of different morphologic spermatozoa (%)																	
Normally formed	0	0	0	0	0	0	0	0	0	0	0	0	0	0	0	0	0
Abnormal head-tail junction	3.9	0.3	1.6	4.2	4.4	0.9	4.1	3.3	0.9	4.3	2.4	1.8	4.8	4.3	1.3	0.4	2.2
Decaudated	0.4	0.0	0.1	0.5	0.4	0.3	0.5	0.1	0.6	0.4	0.8	0.1	0.3	0.8	0.6	0.5	0.1
Acephalic	95.7	99.7	98.3	95.3	95.2	98.8	95.4	96.6	98.5	95.3	96.8	98.1	94.9	94.9	98.1	99.1	97.7

a. "– / –" represents a homozygous nonsense mutation or a splice site mutation that were predicted to cause no protein production. "– / M" represents a compound heterozygous mutation composed of a missense mutation and either a nonsense, or a frameshift, or a splice site mutation that were supposed to remain a mild function of SUN5 protein. "M / M" represents homozygous or heterozygous missense mutations that were supposed to remain some basic function of SUN5 protein. "No MT" represents no mutations identified. **b**. "P" represents proband. **c**. Values are means of semen parameters calculated from more than twice of ejaculated semen analyses. **d.** The unit of concentration is "$\times 10^6$ / ml". Sperm concentration was based on normally formed spermatozoa, abnormal head-tail junction spermatozoa, and decaudated spermatozoa. **e.** Mobility B+C (%) represents the total motility of normally formed spermatozoa, abnormal head-tail junction spermatozoa and acephalic spermatozoa, since no rapid progressive mobility sperm (grade A) was observed in all patients. **Note:** All groups showed oligozoospermia with less than 15×10^6/ml sperm （or 39×10^6 per ejaculate）(the normally formed spermatozoa, the abnormal head-tail junction spermatozoa and the decaudated heads observed in fresh semen were counted as sperm), and asthenospermia (the motility of the normally formed spermatozoa, the abnormal head-tail junction spermatozoa and the acephalic spermatozoa was less than 40%). No sperm showed rapid progressive motility (grade A).

Table S2. Statistical analysis of the semen parameters of the affected individuals according to *SUN5* genotype.

Mutation types	– / – (n = 2)	– / M (n = 4)	M / M (n = 2)	No MT (n = 9)	– / – vs – / M	– / – vs M / M	– / – vs No MT	– / M vs M / M	– / M vs No MT	M / M vs No MT
volume (ml)	2.3 ± 0.5 [a]	2.5 ± 0.6	2.8 ± 0.6	2.6 ± 0.3	0.81 [b]	0.61	0.63	0.78	0.85	0.87
Concentration [a]	5.7 ± 0.8	5.9 ± 2.1	4.3 ± 1.1	4.3 ± 0.8	0.93	0.39	0.30	0.52	0.52	0.96
Motility B+C (%)	23.3 ± 3.1	11.65 ± 3.4	20.9 ± 2.5	13.7 ± 2.7	0.08	0.61	0.11	0.10	0.65	0.26
Percentages of different morphologic spermatozoa (%)										
Normally formed	0	0	0	0	NA	NA	NA	NA	NA	NA
Abnormal head-tail junction	3.7 ± 0.4	2.8 ± 0.9	2.1 ± 1.8	2.5 ± 0.5	0.40	0.53	0.12	0.78	0.79	0.78
Decaudated	0.3 ± 0.2	0.3 ± 0.1	0.2 ± 0.2	0.5 ± 0.1	0.96	0.76	0.49	0.68	0.23	0.22
Acephalic	96.0 ± 0.6	96.9 ± 1.0	97.7 ± 2.0	97.0 ± 0.6[b]	0.46	0.55	0.28	0.77	0.92	0.65

a. Values are expressed as Mean ± SEM. b. P values > 0.05 means the difference between two groups are not significant. NA: not applicable.

Table S3. Filtering of WES variants in two affected individuals F1:II-3 and F2:II-4

	P1	P2
Total variants	102874	111794
After excluding variants reported in dbSNP, 1000 genomes, EVS, Hapmap-CHB and ExAC (MAF > 1%).	1496	1465
Exonic non-synonymous or splice site variants, or coding indels	237	238
Homozygous or compound heterozygous (excluding X and Y chromosomes)	6	5
Homozygous	3	0
In homozygous region > 1Mb	2	-

Table S4 WES homozygous variants that survived filtering in affected individual F1:II-3

Genomic SNV	Gene	Change	phastCons score	ExAC allele frequency	ExAC homozygotes frequency	NNSplice	SIFT	Polyphen	Mutation Taster	OMIM	Homozygous interval
Chr9: 135523687 G>T	*DDX31*	c.1176-5C>A	0[a]	13/120940	0/120940	0.51 to 0.14[b]	-	-	-		0.18 Mb
Chr13: 52249312 G>A	*WDFY2*	c.G212A;p.Cys71Tyr	688	0	0	-	0.00 (D)[c]	**0.962 (D)**	1.000 (D)		3.97 Mb
Chr20: 31573615 G>A	*SUN5*	c.C824T;p.Thr275Met	501	4/121306	0/121306	-	0.00 (D)	**0.999 (D)**	1.000(D)		2.19 Mb

a. phastCons score reveals the conversation of the site. The scores were higher; the possibilities of being deleterious for the variants will be higher. **b**. NNSplice reveals the decrease of the acceptor site score from 0.51 down to 0.14. **c**. Scores were lower in SIFT or higher in either Polyphen or MutationTaster, the possibilities of being deleterious (D) for the mutations will be higher.

Table S5 WES heterozygous variants that survived filtering in the affected individual F2:II-4

Genomic SNV	Gene	Change	phastCons score	ExAC allele frequency	ExAC homozygotes frequency	SIFT	Polyphen	MutationTaster	OMIM
Chr2: 100938293	*LONRF*	c.G263T;p.Gly88Val	0	Not found	Not found	0.11 (T)	0.297 (B)	0.000 (N)[a]	
Chr2: 100938294	*LONRF*	c.G262T;p.Gly88Trp	0	Not found	Not found	0.01 (**D**)	0.957 (**D**)	0.000 (N)	
Chr11: 66307056	*ZDHHC*	c.C799T;p.Pro267Ser	469	Not found	Not found	0.33 (T)	0.994 (**D**)	1.000 (**D**)	
Chr11: 66307057	*ZDHHC*	c.G798T;p.Leu266Phe	469	2/111740	0/111740	0.20 (T)	0.923 (**D**)	1.000 (**D**)	
Chr17:76554252	*DNAH1*	c.G2116A;p.Glu706Lys	0	1/117758	0/117758	1.00 (T)	0.003 (B)	0.000 (N)	
Chr17: 76421553	*DNAH1*	c.A13015G;p.Met4339V	524	6/121214	0/121214	0.19 (T)	0.063 (B)	0.112 (N)	
Chr17: 76421543	*DNAH1*	c.A13025G:p.Lys4342Ar	524	5/121274	0/121274	0.23 (T)	0.191 (B)	0.804 (**D)**	
Chr20: 62191852	*HELZ2*	c.C7480G;p.Leu2494Val	505	16/120832	0/120832	0.34 (T)	0.063 (B)	0.001 (N)	
Chr20: 62196216	*HELZ2*	c.T3959C;p.Leu1320Pro	0	3/117818	0/117818	0.04 (**D**)	0.899 (**P**)	0.000 (N)	
Chr20: 31571674	*SUN5*	c.C1066T;p.Arg356Cys	440	6/121306	0/121306	0.00 (**D**)	0.999 (**D**)	1.000 (**D**)	
Chr20: 31583474	*SUN5*	c.T485A;p.Met162Lys	435	Not found	Not found	0.02 (**D**)	0.042 (B)	**0.778** (**N**)[b]	

a. The letter D in the brackets indicates deleterious, N neutral, T tolerated and B benign. **b.** The p.Met162Lys mutation is predicted to cause a loss of coil in SUN5.

Table S6. Genomic PCR primers used to amplify *SUN5* exons for Sanger sequencing.

Exon	F/R[a]	Primer Sequence (5' to 3')	PCR Size (bp)
1	F	TTGGCACTTTTCAGGGGAC	564
	R	TTGGAATTTCTGTCACCTGCA	
2/3	F	CAACCTGGGTCTTTTCCTTGA	684
	R	CCGATGGGTAGAACTCCAGA	
4	F	AACCAGTGCCCACCTGTAG	391
	R	GGATAGCTTTTCTGGTCTGGC	
5	F	TTGCCAAGTTCACAGGGTTG	489
	R	ACGGTTTGGGGAGAGCTTTA	
6	F	CGCCTTCTTCTCTTTGCCAG	483
	R	TGGATCTGGGTCAAGTCAGG	
7	F	TGTGGGAGAATAGATGGATGAAG	475
	R	TGCAATTAAGGATGCTGCCA	
8	F	ATGAATGGGTCCAGGGATGG	284
	R	AGATGTTTGGGGCAGAATGG	
9	F	GTTAGGGAGAGGACAGCGTC	299
	R	ATGAACTTCCCAGCGGCA	
10	F	ATAGTCAGGGCCCATCAGTG	481
	R	CAAAGCAAGCTGTCCCTCTG	
11	F	AGGGGATCAAAGGTGGGATG	376
	R	ACTTCCAGCCTTAACCAAGC	
12	F	TCTTCAGAGACCATGGAGCC	667
	R	AAGAAACACAGCAAGAGGGC	
13	F	TGTCTGTCCTTCTGGCCTC	437
	R	TCAGATGTGAAAGGCTAGCC	

a. F represents forward primers and R represents reverse primers.

Web Resources

MultAlin, http://multalin.toulouse.inra.fr/multalin/multalin.html;

ESEfinder,

http://rulai.cshl.edu/cgi-bin/tools/ESE3/esefinder.cgi?process=home;

NNSplice, http://www.fruitfly.org/seq_tools/splice.html;

SIFT, http://sift.bii.a-star.edu.sg/;

Polyphen, http://genetics.bwh.harvard.edu/pph2/;

MutationTaster, http://www.mutationtaster.org/